Case Studies in Construction Materials 17 (2022) e01663

Contents lists available at ScienceDirect

Case Studies in Construction Materials

journal homepage: www.elsevier.com/locate/cscm

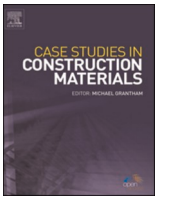

Case study

Material behaviour of unstabilised earth block masonry and its components under compression at varying relative humidity

Philipp Wiehle [a,*,1], Maximilian Brinkmann [b,2]

[a] Bundesanstalt für Materialforschung und -prüfung (BAM), Unter den Eichen 87, 12205 Berlin, Germany
[b] Technical University of Darmstadt, Institute of Concrete and Masonry Structures, Franziska-Braun-Straße 3, 64287 Darmstadt, Germany

ARTICLE INFO

Keywords:
Earth block masonry
Compression tests
Stress-strain relation
Relative humidity
Moisture content
Compressive strength

ABSTRACT

In this study, the material behaviour of unstabilised earth block masonry consisting of different block and mortar types is analysed with particular regard to the influence of varying relative humidity. The uniaxial compressive strength and deformation characteristics of unstabilised earth blocks and mortars as well as of unstabilised earth block masonry are studied in detail and compared to conventional masonry to evaluate whether the structural design can be made accordingly. An increase of 30 % points in relative humidity leads to a reduction of the masonry's compressive strength between 33 % and 35 % whereas the Young's modulus is reduced by 24–29 %. However, the ratio between the Young's modulus and the characteristic compressive strength of earth block masonry ranges between E_{33}/f_k = 283–583 but is largely independent of the relative humidity. The results show that the mechanical properties of the investigated unstabilised earth block masonry are sufficient for load-bearing structures, yielding a masonry compressive strength between 2.3 MPa and 3.7 MPa throughout the range of moisture contents investigated. In general, the design concept of conventional masonry can be adapted for unstabilised earth masonry provided that the rather low Young's modulus as well as the moisture dependence of both, compressive strength and Young's modulus, are sufficiently taken into account.

1. Introduction

Earth is one of the oldest building materials of the world and is more commonly used for load-bearing constructions in developing countries. However, earthen building materials, more precisely earth block masonry, gained in importance over the last decade in developed countries, due to its low environmental impact. Approximately 90 % of all human-made materials are related to building activities, whereas concrete and aggregates contribute the largest share with around 40 % and 35 % respectively followed by bricks with 10 % and asphalt with 5 % [1]. At the end of their life cycle, these materials are usually downcycled and used as inferior components for new materials, leading to a scarcity of resources such as sand or aggregates in general. Furthermore, the building industry causes about 11 % of the global CO_2 emissions, whereas the cement industry contributes the largest share with around 8 % [2]. On the same time, the demand for dwelling steadily increases. According to various estimations a yearly total of 220.000–350.000

* Corresponding author.
E-mail address: philipp.wiehle@bam.de (P. Wiehle).
[1] ORCID: 0000-0002-6485-0173.
[2] ORCID: 0000-0001-9578-313X.

https://doi.org/10.1016/j.cscm.2022.e01663
Received 7 June 2022; Received in revised form 24 October 2022; Accepted 8 November 2022
Available online 11 November 2022

new built dwelling units are needed over the next decade in Germany alone [3–6]. In general, around 73 % of all residential buildings are currently realised as masonry structures and 70 % are erected with a low number of storeys containing only one or two dwelling units [7]. Thus, the majority of new residential buildings does not have to be constructed with high strength materials such as reinforced concrete or fired bricks. The numbers given can at least be extrapolated to the European market. CO_2 emission as well as energy and resource consumption of the construction industry are one determining factor of the human-made climate change, thus a rethink must take place envisaging the use of environmental-friendly and completely recyclable building materials such as unstabilised earth. However, the knowledge of the material and load-bearing behaviour of unstabilised earth block masonry is still limited and thus the possible application cases are severely restricted. This is why only a few design guidelines for load-bearing earth constructions exist [8], which often include strict and generalised limitations concerning the minimum wall thickness, storey height or the number of storeys [9]. Particularly the influence of ambient climate conditions on the material behaviour and its strength and deformation characteristics is not yet sufficiently researched. Compressive strength and Young's modulus of unstabilised earth block masonry materials decrease, if the material moisture content is increasing. The characteristic of the decrease is influenced by the material composition as it is shown in a previous study [10]. Heath et al. [11] describe the influence of the material moisture content on the compressive strength of unstabilised extruded earth blocks by means of an exponential function. The variation in strength normalised by strength at a moisture content of 1 % by mass delivers a generally valid approach. The relation of the strength and deformation characteristics to the moisture content is well established and suitable in case of earth blocks or mortars. However, in terms of masonry specimens this is hardly feasible due to their large size and the fact that the moisture content depends on the equilibrium moisture content of the blocks and the mortar and their ratio in the masonry bond. The masonry's mechanical parameters more conveniently could be related to the ambient climate conditions after storing until equilibrium weight is reached. Using the relative humidity (RH) as a generally valid reference parameter also seems to be reasonable with regard to the structural design. The moisture content of earth block masonry distinctively depends on its application case and will for example be considerably smaller at an interior wall compared to an exterior wall. Thus, the definition of application classes in dependence of the RH following the approach for timber structures in EN 1995 [12] is expedient in order to consider the actual moisture content in the best possible way. To do so, the masonry compressive strength needs to be related to RH rather than to the material moisture content, which is a material specific parameter and may vary for different masonry types at the same level of RH.

The mechanical parameters of blocks and mortars as a consequence ought to be related to RH as well.

A possible procedure is defined in the German standard for testing of earth blocks DIN 18945 [13], where the blocks are conditioned at 50 % RH until they reach equilibrium weight prior to testing and subsequently categorised in compressive strength classes. Since the relative reduction in compressive strength with increasing RH is comparable for different block types [10], the initial mechanical properties of the masonry can be adapted accordingly.

However, there is a lack of actual compression tests on unstabilised earth block masonry at varying ambient climate conditions to verify these relations.

Only a few studies deal with the compressive strength of unstabilised earth block masonry. Müller et al. [14] showed that the material and load-bearing behaviour of unstabilised earth block masonry made of hand- moulded or extruded blocks at constant climate conditions (23 °C/ 50 % RH) is in general comparable to conventional masonry made of aerated autoclaved concrete (AAC), fired bricks or calcium silicate units. The compressive strength reported ranges between 1.99 and 3.67 MPa and the Young's modulus lies between 783 and 1367 MPa. The E_{33}/f_k ratio accordingly ranges between ~430 and ~500.

Miccoli et al. [16,17] conducted compression tests on unstabilised earth block masonry specimens after conditioning at 23 °C and 50 % RH. The bed joint width in this case amounted to ~20 mm to better describe the material behaviour of ancient earth block masonry constructions, which was the aim of this study. The mean compressive strength of the masonry is 3.28 MPa and the Young's modulus amounts to only 803 MPa as a result of the fairly wide bed joints. The E_{33}/f_k ratio in this case amounts to ~245.

Heath et al. [18] conducted compressive strength tests on six masonry specimens erected with unstabilised extruded earth blocks after conditioning at 20 °C and 62.5 % RH. The average compressive strength is 2.49 MPa and as expected lower than the unit strength tested at the same RH. A conditioning time or a criteria to determine the testing date is not defined. As a result of these studies, the load-bearing behaviour of unstabilised earth block masonry in general is comparable to conventional masonry. However, the influence of RH on the material and load-bearing behaviour of unstabilised earth block masonry by actual testing at varying ambient climate conditions is not known so far.

It seems to be reasonable to carry out the structural design of unstabilised earth block masonry under compression loading in accordance with the structural design of conventional masonry in compliance with Eurocode 6 [15] whereas some adaptions are mandatory. Especially for slender walls, the rather low Young's modulus E_{33} of unstabilised earth block masonry needs to be taken into account. Extended second order effects will occur under compression loading and distinctively affect the load-bearing capacity. Thus, the Young's modulus hast to be investigated and adequately considered to prevent stability failure. Besides, the masonry compressive strength depends on the ratio of the transversal strain of block and mortar. The influence of the moisture content on the transversal strain of both, blocks and mortars thus needs to be investigated.

The scope of the present study is to investigate the material behaviour of unstabilised earth block masonry and its components in detail. Earth blocks and mortars as well as the masonry are tested according to common masonry testing standards to obtain values that are comparable to those of conventional masonry. To illustrate the influence of the moisture content on the material behaviour three different ambient climate conditions are chosen for conditioning of the samples prior to testing. The mechanical parameters determined in this study are directly related to the RH of the conditioning climate. Sorption isotherms of the blocks are given to relate RH and material moisture. Two types of unstabilised earth blocks, significantly differing in material composition and production method, are examined to illustrate the spectrum of the material properties of merchantable load-bearing earth blocks. Additionally, two types of

unstabilised earth mortars are investigated to extent the variety of block-mortar combinations for masonry specimens and to study the influence of the mortar on the material and load-bearing behaviour of masonry exposed to varying RH. Finally, the characteristic mechanical parameters are compared to conventional masonry to facilitate the interpretation of the findings.

2. Experimental programme

2.1. Materials and sample preparation

The examined unstabilised earth blocks and unstabilised earth block masonry mortars are industrially manufactured and declared as load-bearing according to German Standards DIN 18945 [13] and DIN 18946 [19]. One block is an extruded perforated block with a size of 240 × 175 × 113 mm^3 which corresponds to the triple-thin-format (3DF) according to the German masonry block formats and thus will be labelled 3DF in this study. The second one is a hand moulded block measuring 240 × 115 × 71 mm^3, corresponding to the German normal format and will be designated NF in the following. The bulk density of the NF block is 1789 kg/m^3 and amounts to 1874 kg/m^3 in case of the 3DF block. Both blocks contain grains up to a maximum size of 4 mm, whereas the grain size distributions are largely similar with differences in the clay and gravel fractions (Table 1).

The NF block contains ~3 % of wood chaff and the 3DF block ~6 % of cellulosic fibres. Illite, vermiculite, chlorite and muscovite were identified by means of X-ray diffraction analyses. Both mortars are pre-mixed dry mortars of different compressive strength classes. The bulk density of the mortar complying with compressive strength class 2 (M2) is 1950 kg/m^3, the mortar corresponding to compressive strength class 3 (M3) yields 1960 kg/m^3. The grain size distribution of both mortars is also largely similar, showing differences in the clay and silt fractions (Table 1). The content of organic matter amounts to 2 % in case of the M2 mortar and 1 % in case of the M3 mortar. Illite and muscovite are present in both mortars, chlorite in addition was identified in the M3 mortar. Fig. 1.

To illustrate the influence of the material moisture, the experimental tests are conducted after conditioning in three different ambient climate conditions with a constant temperature of 23 °C and RH of 50 %, 65 % and 80 %. All prepared block, mortar and masonry specimens were stored in climate chambers at the respective climate conditions until they reached mass equilibrium, which was defined by a maximum weight variation of 0.1 wt% in 24 h in contrary to DIN 18945 [13] and DIN 18946 [19], where 0.2 wt% are specified.

Earth block specimens for uniaxial compressive strength tests were prepared according to the respective standard [13]. The earth blocks in NF format were cut in half and stack-bonded with opposite cut surfaces by means of a thin layer of gypsum. The 3DF blocks were tested as whole blocks. To ensure plano-parallel surfaces for load introduction, the specimens were levelled with a thin gypsum layer on top and bottom side.

In contrary to the compressive strength, the Youngś modulus of the blocks was determined using masonry prism specimens of three stack-bonded blocks according to Schubert [20]. This test set-up enables deformation measurements in the mid-third of the samples, without distinct restraints of transversal strains.

Earth mortars were adjusted to a spread flow diameter of 175 mm according to DIN 18946 [19]. Mortar prisms of 100 × 100 × 200 mm^3 according to DIN 18555-4 [21] were prepared for axial and transversal strain measurement. After desiccation, the specimens were levelled with a thin gypsum layer on top and bottom side.

The masonry wallettes were prepared according to DIN EN 1052-1 [22] by laying five (3DF) or six (NF) block courses on bed joints of ~12 mm. The head joints were completely filled with mortar. The samples were erected in single-leaf construction with pre-wetting of all joint contact surfaces by submerging the blocks into water of ~10 mm for approximately 5 s. Load introduction beams were attached on top and bottom side by a thin gypsum layer to ensure plano-parallel load introduction.

2.2. Experimental set-up

2.2.1. Blocks and mortar

The experimental determination of the compressive strength of the blocks was carried out with a force-controlled loading rate, that evokes failure after 30–90 s. The Youngś modulus was determined after three load-unload cycles up to 1/3 of the maximum stress according to DIN 18945 [13]. The tests were conducted using a 1 MN universal testing machine and axial and transversal displacements were measured continuously with two clip-on extensometers each. The test set-up of the compressive strength as well as the deformation measurement is depicted in Fig. 2. The deformation characteristics of the mortars were measured following the procedure defined in DIN 18555–4 [21]. The loading scheme in contrary, was adapted from [13], to be able to compare transversal strains of blocks and mortars. The low loading rate and the unicyclic load scheme given in [21] includes long-term effects, which are not existent

Table 1
Grain size distributions of blocks and mortars.

Sample	clay (d < 0.002 mm) (wt%)	silt (0.002–0.063 mm)	sand (0.063–2 mm)	gravel (d > 2 mm)
3DF	16.05	43.90	34.82	5.23
NF	10.33	46.63	42.54	0.50
M2	6.67	26.28	66.00	1.05
M3	4.13	30.37	64.16	1.34

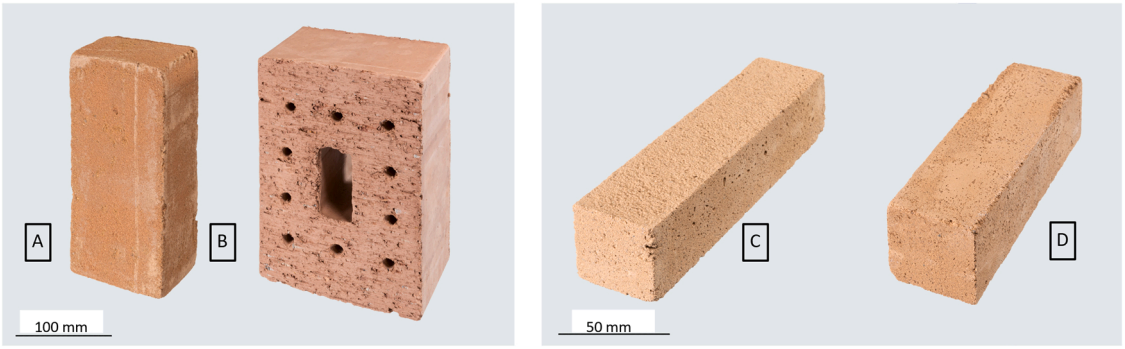

Fig. 1. Hand moulded earth block in NF format (A), extruded perforated earth block in 3DF format (B), prisms of M3 (C) and M2 (D) mortar.

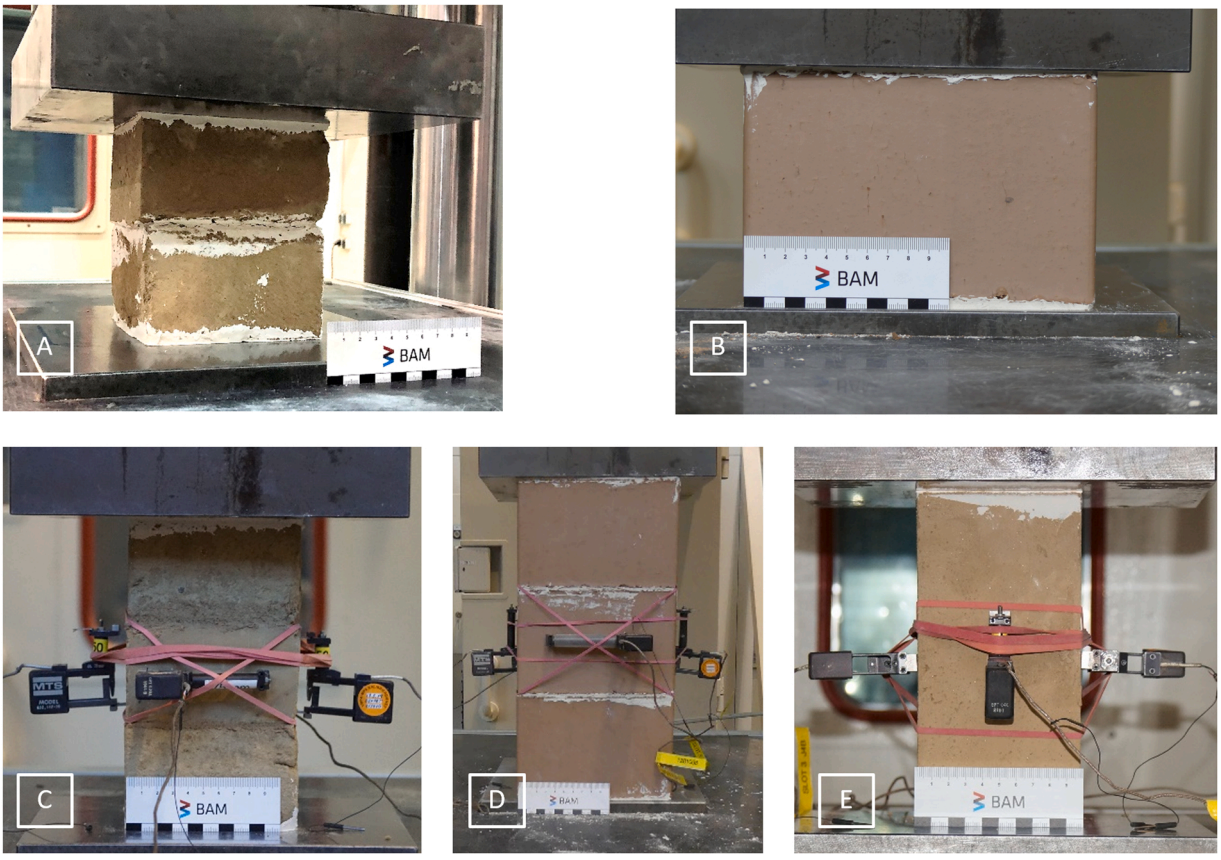

Fig. 2. Test set-up for the determination of the compressive strength of NF blocks (A) and 3DF blocks (B) and axial and transversal strains of NF blocks (C) and 3DF blocks (D) as well as compressive strength and deformations of the mortars (E).

in case of of the block tests. The transversal strain ratio of blocks and mortar is known to be a crucial factor of the masonry's compressive strength. The compressive strength of the mortars was determined in a final load cycle up until failure after the determination of the Young's modulus. Per climate condition, a total of ten earth block samples were used for compressive strength tests and three samples of blocks and mortar each to determine the Young's modulus.

To relate the RH of the conditioning climate with a corresponding material moisture, the sorption isotherms of the blocks were determined using a Gravisorp 120 multisample dynamic vapour sorption (DVS). The sorption isotherms given are averaged from the ad- and desorption branch. and were recorded from 0 % RH – 95 % RH in steps of 5 % at a constant temperature of 23 °C.

2.2.2. Masonry

The compression tests were carried out on a 1 MN universal testing machine under displacement-controlled loading according to

DIN EN 1052–1 [22]. The load rate ranged between 0.2 and 0.3 mm/min and thus failure occurred after 15–30 min. Displacements were monitored continuously by two linear variable differential transformers (LVDTs) parallel and one LVDT perpendicular to the loading direction on each side. The test set-up is shown in Fig. 3. The uniaxial compression tests were conducted for all four combinations of blocks and mortars. Three specimens per block-mortar-combination were tested at every RH level, which results in a total of 36 compression tests on masonry wallettes.

2.3. Test results

2.3.1. Earth blocks and mortar

The results of the compression tests of the blocks and mortars including the standard deviation are summarised in Table 2. Compressive strength and Young's modulus and of both, blocks and mortars, decrease with increasing RH. The compressive strength f_b of the blocks ranges between 3.55 and 5.38 MPa (3DF) and 3.30 and 4.38 MPa (NF). The compressive strength f_m of the mortars vary between 2.92 and 4.13 MPa.

At failure, the block samples of the compressive strength tests showed vertical cracks along the fringes whereas the NF samples exhibited some cracks in the middle (Fig. 4 (A) and (B)). The failure of the NF and 3DF prisms for deformation measurement is visible by a vertical crack in the specimen's centre (Fig. 4 (C) and (D)). The mortar prisms show diagonal cracks (Fig. 4 (E)).

Fairly low scattering can be observed in case of the compressive strength of blocks and mortars, while the Young's modulus scatters more widely. The Poisson ratio of the mortars exhibits no clear dependence on RH and is in the same range for both. The Poisson ratio of the NF blocks, in contrary, is decreasing with increasing RH. In terms of the 3DF blocks the values are fairly high at 50 % and 65 % RH. However, the tendency of decreasing Poisson ratio with increasing RH is also existent (Table 2). The moisture content of the samples at the respective RH level is given via the sorption isotherms depicted in Fig. 5.

2.3.2. Masonry

The compressive strength and Young's modulus of the earth block masonry show a similar behaviour as block and mortar samples when exposed to varying climate conditions as they decrease with increasing RH. The compressive strength f of the masonry samples ranges between 2.27 and 3.72 MPa and the Young's modulus E_{33} varies between 592 and 1656 MPa. By comparing the results given in Table 3, it becomes obvious that the different kinds of mortar only slightly influence compressive strength and Young's modulus of the masonry samples.

The reason for this is that both investigated mortars have very similar mechanical properties and thus the results of the masonry samples in Fig. 6 and in the following considerations are combined per block type neglecting the influence of the different mortars. The moisture content of the masonry samples was not explicitly determined, but since the block's presence is dominant in the masonry bond, their sorption isotherms reported in Fig. 5 can be used in good approximation.

Again, the scatter of the compressive strength is remarkably low and slightly higher in terms of the Young's modulus. The Poisson ratio of the NF masonry ranges between 0.09 and 0.18 which reflects the values measured on the blocks. The 3DF masonry, especially the combination of 3DF blocks and the M3 mortar, in contrary exhibits fairly low Poisson ratios compared to the blocks (Table 3).

Failure of the masonry occurs ductile with a pronounced post-peak softening phase. The failure patterns show vertical cracks above and beneath the head joints and mortar spallings in the bed joints at the front and rear surfaces, whereas shell-formed spallings induce

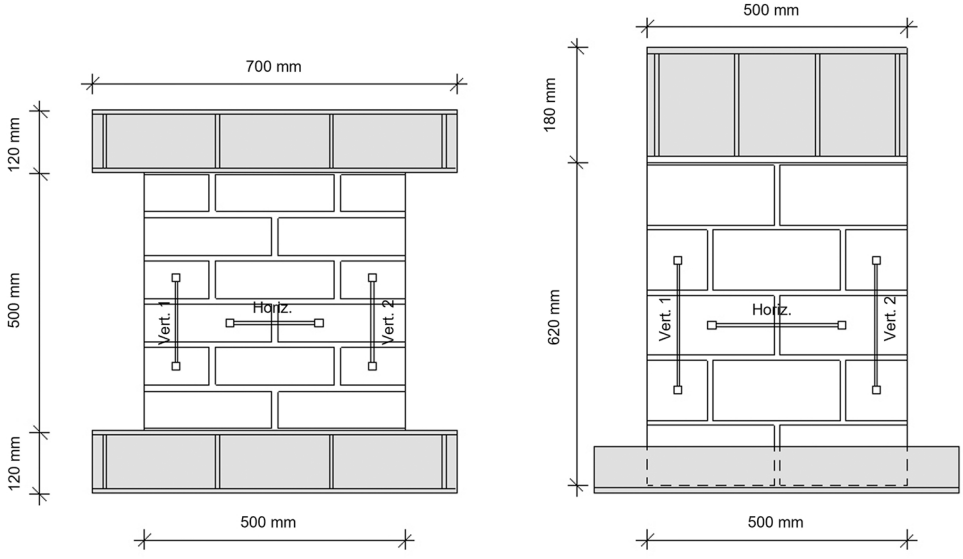

Fig. 3. Test set-up of the masonry wallets including measuring sections of NF (left) and 3DF (right) specimens.

Table 2
Compressive strength and Youngś modulus of NF and 3DF blocks as well as M2 and M3 mortar depending on RH.

Block/mortar	RH (%)	compressive strength f_b (MPa)		Youngś modulus E_{33} (MPa)		Poisson ratio ν_{33} (dimensionless)
		Mean	STD	Mean	STD	Mean
NF	50	4.38	0.26	2735	219	0.17
	65	4.03	0.14	2167	95	0.13
	80	3.30	0.11	1629	69	0,10
3DF	50	5.38	0.18	3222	662	0.44
	65	4.30	0.06	3017	80	0.52
	80	3.55	0.10	1589	61	0.19
M2	50	4.13	0.13	5699	273	0.10
	65	3.74	0.06	4421	264	0.11
	80	3.10	0.01	3028	983	0.10
M3	50	4.08	0.03	5419	260	0.13
	65	3.79	0.04	5139	169	0.12
	80	2.92	0.03	4112	523	0.14

Fig. 4. Cracking patterns of compressive strength samples of NF blocks (A) and 3DF blocks (B) and of NF (C) and 3DF (D) prisms used for deformation measurement as well as cracking patterns of the mortar prisms (E).

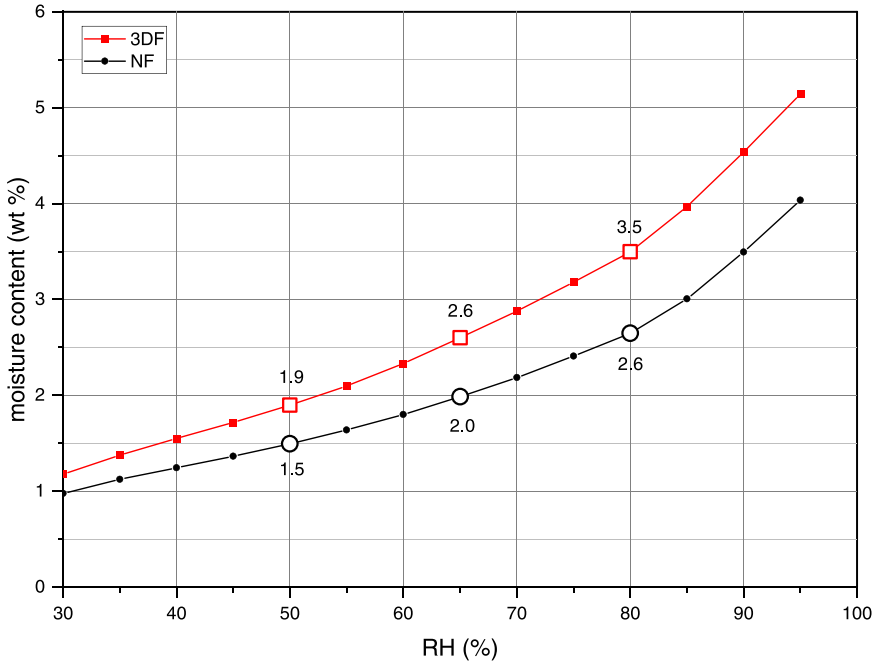

Fig. 5. Sorption Isotherms averaged from ad- and desorption branch of NF- and 3DF blocks at 23 °C highlighting the mean moisture content at testing/conditioning climates.

Table 3
Summary of the masonry test results depending on RH.

Specimen	RH (%)	Quantity	Compressive strength f (MPa)		Young's modulus E_{33} (MPa)		Poisson ratio ν_{33} (dimensionless)
Block/mortar			Mean	STD	Mean	STD	Mean
NF/M2	50	3	3.72	0.14	1656	115	0.18
	65	3	3.12	0.10	1454	410	0.14
	80	3	2.51	0.08	1093	119	0.09
NF/M3	50	3	3.66	0.23	1399	55	0.09
	65	3	3.02	0.13	1528	50	0.14
	80	3	2.43	0.11	1225	147	0.11
3DF/M2	50	3	3.58	0.01	878	78	0.11
	65	3	2.71	0.01	712	169	0.12
	80	2	2.36	0.08	597	8	0.10
3DF/M3	50	3	3.56	0.12	807	152	0.05
	65	3	2.65	0.02	642	67	0.03
	80	2	2.27	0.03	592	77	0.10

a cone shaped crack pattern at the head sides (Fig. 7).

2.4. Evaluation and comparison of results

2.4.1. Blocks and mortars

The compressive strength of blocks and mortars obtained at 80 % RH are consistently above 2.5 MPa which is on the one hand the minimum value for load-bearing mortars and on the other hand the mean value of the compressive strength class 2 for blocks according to DIN EN 1996–1–1/NA [15,23]. Furthermore, the scatter of the compressive strength is fairly low and thus never exceeds the threshold of a coefficient of variation of 25 % as defined in the standard.

The 3DF blocks exhibit constantly higher compressive strength and Young's moduli compared to the NF blocks (Table 2). Reason for this is the higher clay mineral content of the 3DF block as reported in [10]. In Fig. 8 the compressive strength and Young's modulus normalised by the respective values at standard climate conditions according to DIN 18945 [13] (23 °C/ 50 % RH) are given. The decrease in strength and stiffness with increasing RH of the 3DF blocks is slightly higher compared to the NF blocks. In the range between 50 % and 80 % of RH, the compressive strength of the 3DF blocks is reduced by 34 % whereas the Young's modulus is reduced by 50 %. The NF blocks reduction in compressive strength amounts to 25 % and the Young's modulus decreases by 40 %. The test results of both blocks are in accordance with the results obtained for cylinders of the same materials at a broader range of RH [10], which are

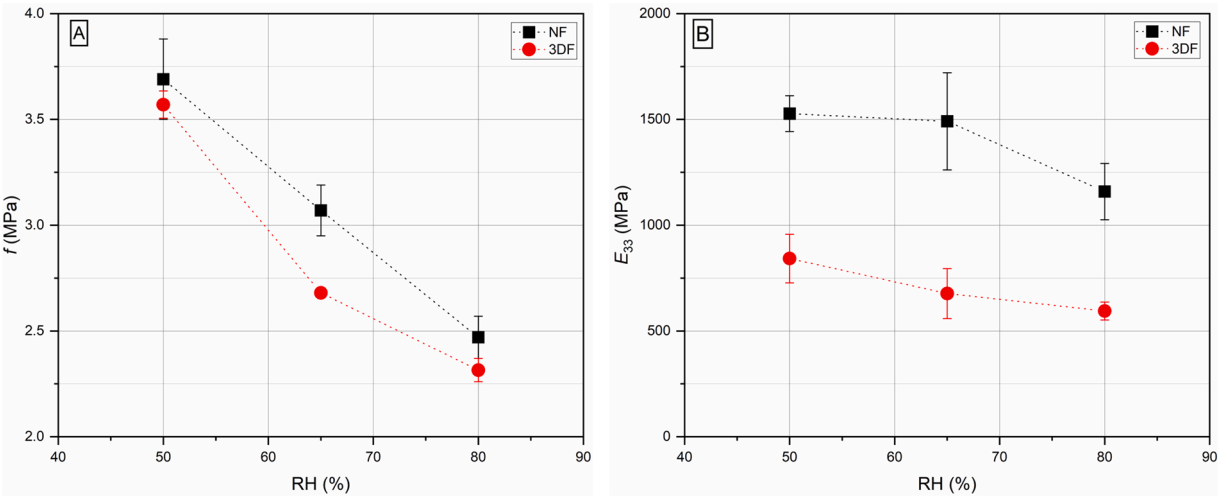

Fig. 6. Compressive strength f (A) and Young's modulus E_{33} (B) of masonry samples per block type depending on RH.

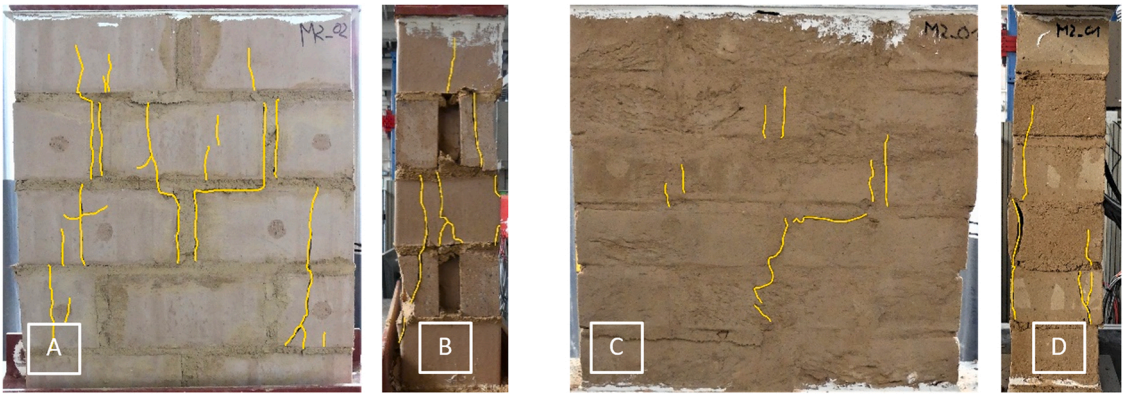

Fig. 7. Crack patterns of masonry samples; front/rear side (A) and head sides (B) of 3DF masonry and front/rear side (C) and head sides (D) of NF masonry.

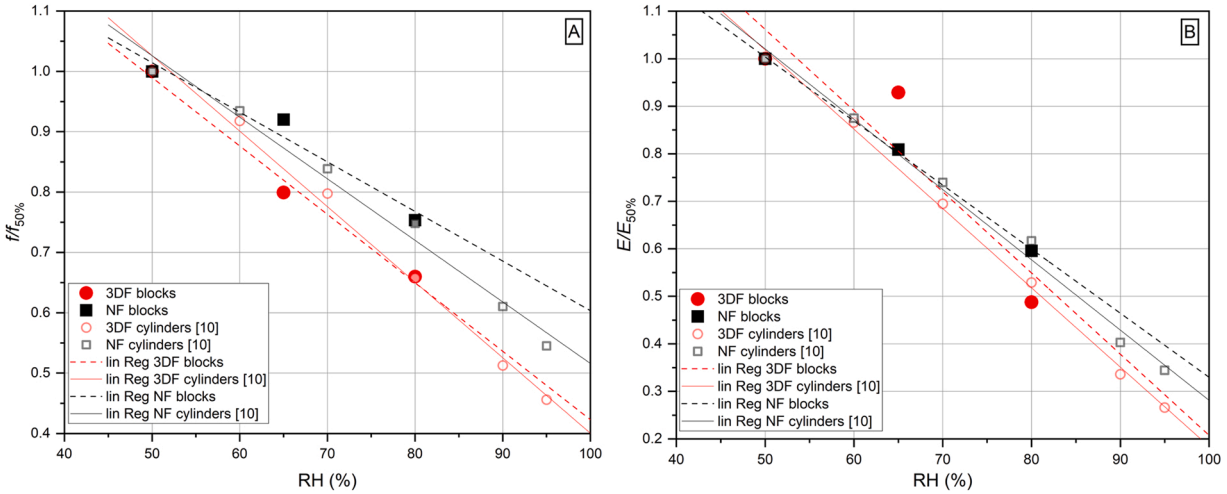

Fig. 8. Normalised compressive strength (A) and Young's modulus (B) of 3DF and NF blocks depending on RH in comparison to normalised results of 3DF and NF cylinders reported in [10].

also included in Fig. 8. The data obtained in case of the cylindric specimens validates the assumption of a linear correlation between RH and compressive strength as well as Youngś modulus.

In Fig. 9 the stress-strain relations of the final load cycle of one 3DF and one NF block as well as for one M2 and one M3 specimen are exemplarily depicted at a RH of 50 % and 80 %. The stress-strain behaviour of both, blocks and mortars, exhibits a largely linear evolution up to approximately 1/3 of the maximum stress. Subsequently the material behaviour is distinctively non-linear. It can be seen that the decrease of compressive strength and Youngś modulus in the range between 50 % and 80 % RH is more pronounced in case of the 3DF blocks. It can also be observed that the fracture strain of the 3DF blocks increases with increasing RH but is regardless of RH in case of the NF blocks. This again is in accordance with the results from cylindric specimens in [10]. The progression of the stress-strain relation is almost congruent for both mortars. The transversal strain of the M3 mortar is slightly higher than of the M2 mortar at RH of 50 %. The ultimate transversal strain is independent of RH in case of the blocks, but significantly increases in case of both mortars.

A closer look at the stress-strain diagrams of the cyclic loading in Fig. 10 provides additional information about the behaviour of the tested materials, in particular, the differences concerning the Poisson ratios given in Table 2. The load path of the first cycle is largely linear for the NF block and the M3 mortar, whereas the 3DF block exhibits a non-linear evolution from the beginning. At the end of the first cycle, a distinctive residual strain can be observed which is more pronounced in case of the 3DF block compared to the NF block and the mortar. The second load cycle also shows a load-unload hysteresis, whereas the residual strain at the end is hardly increasing. During the following retention period of 30 s a negative elastic strain progression can be observed. This is also existent at the following retention period of 30 s at 1/3 of the maximum stress. The strain progression is again more pronounced in case of the 3DF block in comparison to the other materials. Although, a noticeable plastic deformation exists at the end of the first cycle, the curves of the following load cycles including the fracture cycle return to the same strain level as the first cycle for the NF block and the mortar. The evolution of the 3DF blocks curves in contrary shows increasing strains for the second cycle and the fracture cycle. The 3DF block apparently undergoes a pronounced microstructural change which leads to material compaction during the cyclic loading. Moreover, this is the reason for the breaking point of the fracture cycle. After reaching the load level of the three previous cycles, the breaking point constitutes the beginning of another microstructural material state with a lower Youngś modulus.

These observations can be transferred to the evolution of the transversal strain, whereas the 3DF block yields comparatively high values. The fairly high transversal strain is also the reason for the high Poisson ratios of the 3DF blocks (Table 2). The Poisson ratio ν_{33} again depends on RH for both blocks in contrary to the mortars. The decrease of ν_{33} can be explained by the stress-strain relation of the blocks at 80 % RH, which is included in Fig. 10. The transversal strain at 80 % RH stays almost the same, whereas the axial strain increases, thus the ratio decreases with increasing RH. A similar although less pronounced tendency was observed in case of the NF blocks and cannot be seen in case of the mortars.

Due to the elasto-plastic material behaviour of blocks and mortars, the determination of the deformation characteristics depends on the load cycle and yields distinctive differences. In Fig. 11 a comparison of Youngś modulus and Poisson ratio ν_{33} is given exemplarily for both blocks and the M3 mortar. The values were determined for each of the three load cycles and additionally for the third cycle including the retention period at 1/3 of the maximum stress according to DIN 18945 [13]. It becomes apparent, that the Youngś modulus of the first cycle and the third cycle including the retention period are nearly identical for both blocks. This arises from the fact, that the residual strain after the first cycle corresponds to the strain progression during the 30 s retention period at 1/3 of the maximum stress. The Poisson ratio of all materials yields a higher value at the first cycle and stays constant during all following cycles. This behaviour is most pronounced in case of the 3DF blocks. Reason for this is that the slightly higher ratio of plastic deformation of the transversal strain after the first load cycle in comparison to the axial deformation. Furthermore, the Youngś modulus of the mortar exhibits these observations in a less pronounced manner, because the residual axial strain after the first cycle yields comparatively higher values as the strain progression at 1/3 maximum stress (Fig. 10).

To sum up, blocks and mortars exhibit a behaviour under cyclic loading that is typical for elasto-plastic material. The outlined

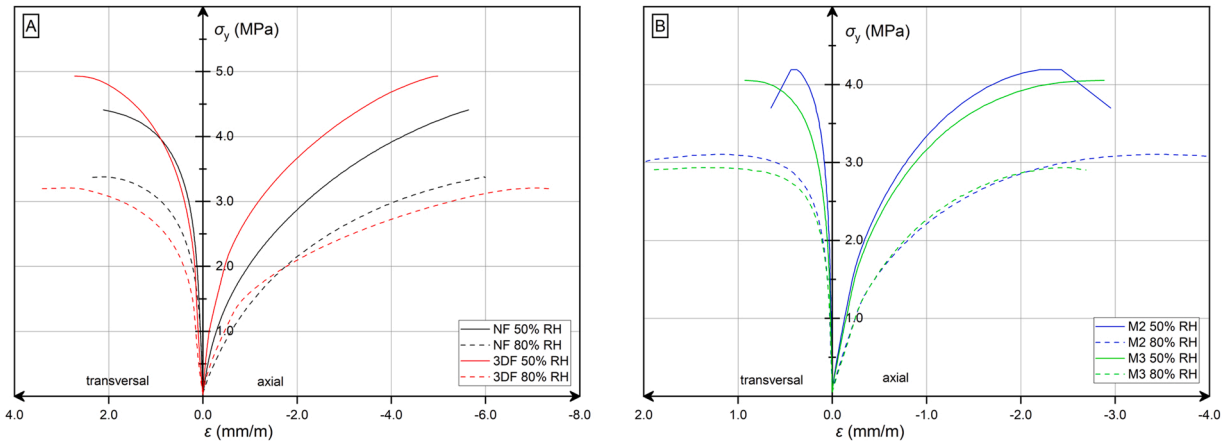

Fig. 9. Comparison of the stress-strain curves of 3DF and NF blocks (A) and of M2 and M3 mortar (B) at 50 % and 80 % RH.

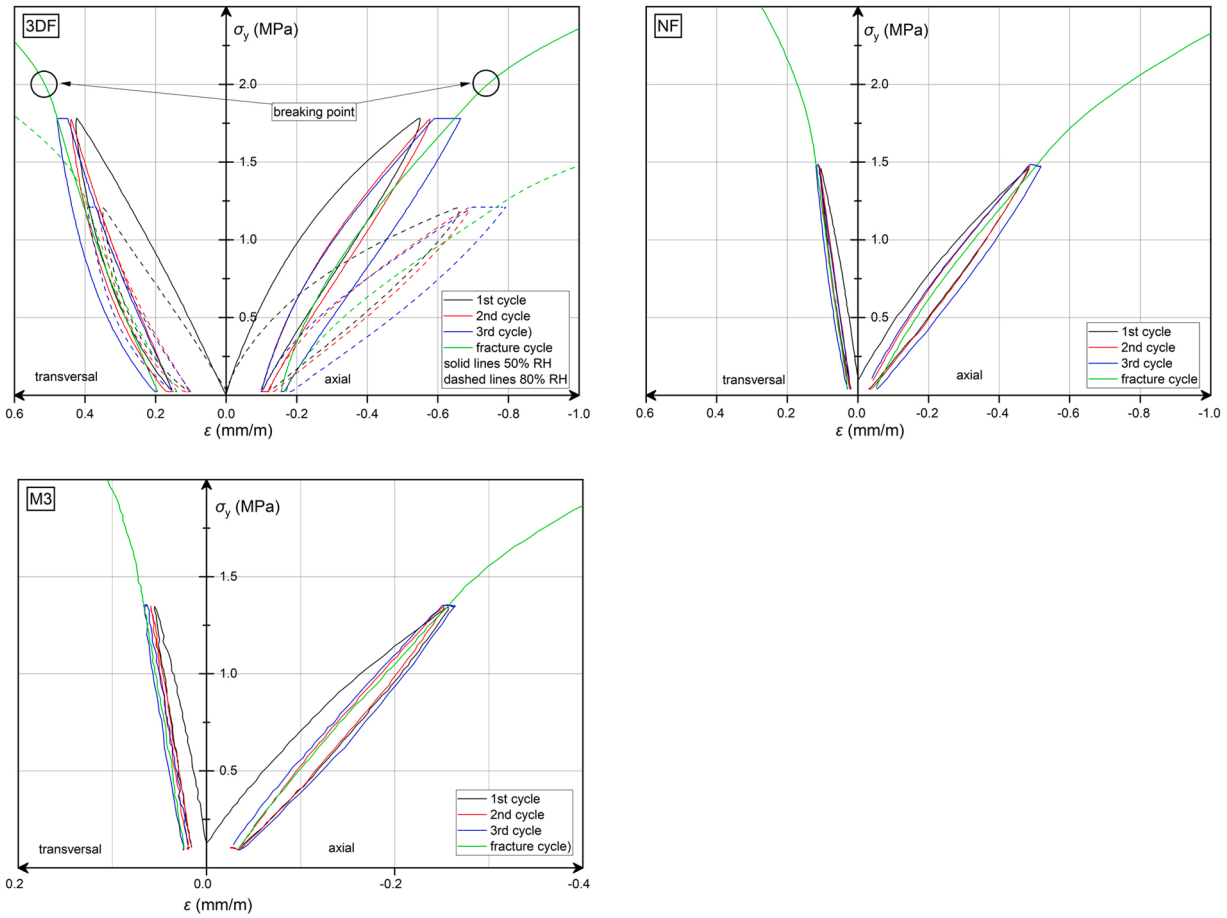

Fig. 10. Exemplary comparison of the stress-strain diagrams of NF blocks and M3 mortar under cyclic loading at 50 % RH and of 3DF blocks at 50 % and 80 % RH highlighting the breaking point of the final load-cycle.

differences between the Young's modulus and the compressive strength of the tested materials can primarily be explained by the material composition, more precisely the clay mineral content as reported in [10]. Moreover, the differences in the stress-strain behaviour between the 3DF blocks and the other materials are influenced by the production method. The extrusion causes a predominant parallel orientation of the clay minerals in axial direction of the blocks which is known to be typical in case of extruded masonry units [24–26]. The transversal deformation under compression loading is possibly influenced by a facilitated gliding of the plate-like mineral elements in load direction. The gliding results in a delamination of the material and increases the transversal strain. This effect could explain the rather high transversal strain values and the distinctive reduction of the Poisson ratio between the first and the subsequent load cycles in case of the 3DF blocks. The NF blocks and the mortar in contrary exhibit a less anisotropic strain behaviour because of the random orientation of the clay minerals in the matrix.

2.4.2. Masonry

The compressive strength and Young's modulus of the masonry specimens essentially reflect the results of blocks and mortar. As mentioned in Section 2.3.2 the mortar type in this case only slightly influences the masonry strength, thus the results are combined per block type in Table 4. The strength values at 80 % RH are still within the range of low strength masonry [15,27]. In contrary to the blocks, the compressive strength of the masonry samples is more affected by increasing RH than the Young's modulus. An increase of 30 % points in RH leads to a decrease of the masonry's compressive strength of 33 % (NF) and 35 % (3DF) while the Young's modulus decreases 24 % (NF) and 29 % (3DF). In case of the blocks, the reduction amounts to 25 % (NF) and 34 %/3DF) in compressive strength and 40 % (NF) respectively 50 % in Young's modulus. The reduction in compressive strength is similar for masonry and blocks in case of the 3DF block and slightly higher for masonry in case of the NF blocks, whereas the reduction of the masonry's Young's modulus is significantly lower than it is in case of the blocks. One reason for this is the triaxial stress state of the mortar in the bed joint, that leads to a constraint of the block's transversal strain and thus a rather low axial strain in comparison to the block specimens, where only a thin layer of gypsum is applied.

Both masonry types exhibit a similar stress-strain behaviour. The 3DF masonry exhibits an initial compaction phase up to approximately 0.5 MPa which results in a lower gradient at the beginning of the stress-strain curve that is increasing subsequently. A

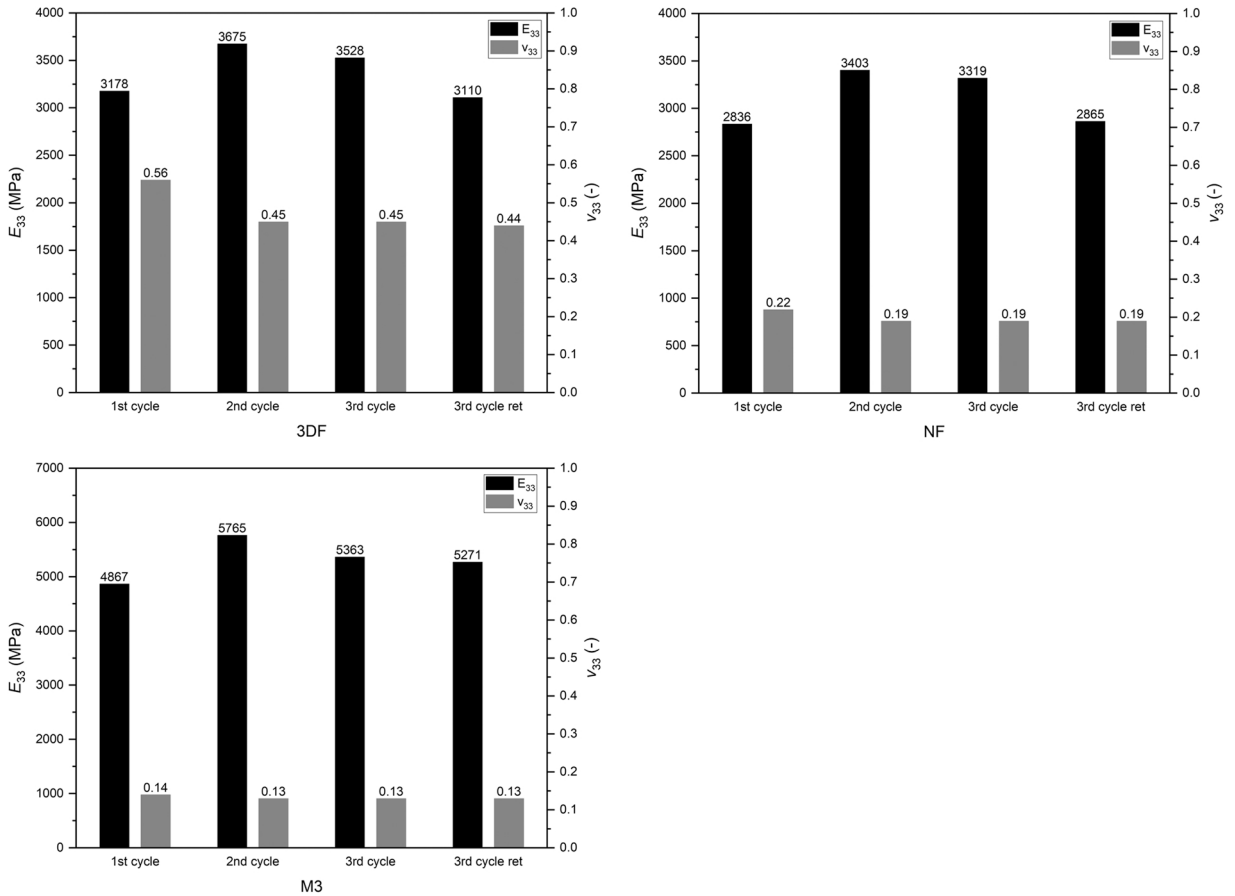

Fig. 11. Comparison of Youngś modulus E_{33} and Poisson ratio ν_{33} of 3DF and NF blocks and M3 mortar depending on the load cycle at 50 % RH.

Table 4
Compressive strength and Youngś modulus of earth block masonry combined per block type.

Masonry	RH (%)	Quantity	Compressive strength f_c (MPa)		Youngs'Modulus E_{33} (MPa)	
			Mean	STD	Mean	STD
NF	50	6	3.69	0.19	1528	85
	65	6	3.07	0.12	1491	230
	80	6	2.47	0.10	1159	133
3DF	50	6	3.57	0.07	843	115
	65	6	2.68	0.02	677	118
	80	4	2.32	0.06	595	43

nearly linear evolution of the axial stress is observed until approximately 1/3 of the maximum stress in case of both masonry types. The following development of the stress-strain relation is clearly non-linear with a rather ductile post peak strain softening phase, whereas the 3DF masonry yields significantly higher strain at ultimate stress. The influence of RH on the stress-strain relations of 3DF and NF masonry is illustrated in Fig. 12. The averaged curves of all six samples per RH and block type are highlighted in bold lines to ensure better clarity. Increasing RH leads to a flattening of the curves and to an increase of the strain at maximum stress. The pronounced initial compaction as well as the comparatively high axial strain of the 3DF masonry is existent at all RH levels.

The transversal strain at maximum stress exhibits no clear dependence on RH. This arises from the fact, that the transversal strain in the upper load section is caused by the development and propagation of vertical cracks which exhibit a similar width for any RH. However, the comparison of the transversal strain at 1/3 maximum stress illustrates a similar, although less pronounced tendency of increasing strain with increasing RH.

In contrary to the NF blocks and masonry, the Poisson ratio of 3DF blocks and masonry significantly differs (Tables 2 and 3). The Poisson ratio in general is defined as the ratio of transversal to axial strain and is determined at 1/3 of the maximum stress. In case of the 3DF masonry, the axial strain is rather high compared to the NF masonry due to the initial compaction, which results in a lower Poisson ratio. The determination of the blocks Poisson ratio is made after cyclic loading and thus includes no axial deformation caused

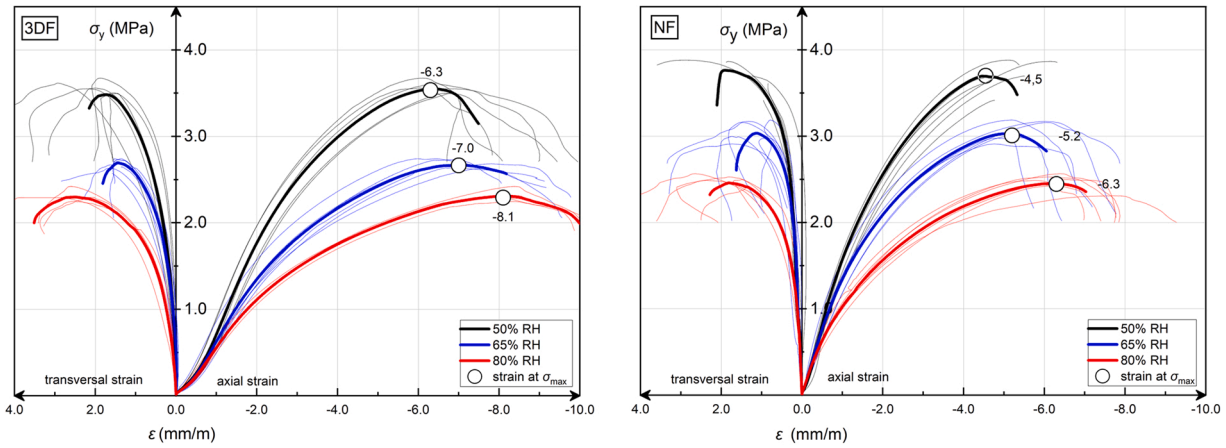

Fig. 12. Stress-strain diagrams of centrically loaded masonry samples depending on RH for 3DF and NF masonry.

by compaction and thus leads to significantly lower Poisson ratios.

2.5. *Comparison of earth block masonry and conventional masonry*

To facilitate the interpretation of the material behaviour of earth blocks, mortars and masonry, an exemplary comparative classification of material parameters is presented in the following. Therefore, units made of calcium silicate and aerated autoclaved concrete (AAC) are chosen as benchmark. The former is considered because of the similar non-linear stress-strain behaviour including post peak strain softening (Fig. 13) and the latter is included because of the similar range of the strength and deformation parameters. In Table 5 the material parameters of earth blocks and mortars obtained at 50 % and 80 % RH are compared to the parameters of calcium silicate and AAC units as well as a M2.5 cement mortar extensively studied in [27].

The conducted tests have shown that the load-bearing behaviour of earth block masonry is essentially equivalent to conventional masonry. Failure is induced by exceeding the tensile strength of the blocks and consequently accompanied by vertical cracks mainly above and beneath the head joints. The shell-formed spallings of the blocks that can be observed on both front sides (Fig. 7), are more frequent for 3DF masonry and correspond to the failure of fired bricks. Main reason for this is the preferred orientation of the plate like clay minerals during extrusion [24–26]. A significant difference is the prominent initial compaction phase of the 3DF masonry. This causes a comparatively low Youngś modulus, although the gradient of the stress-strain curves of 3DF and NF masonry is comparable. However, the respective standard for masonry compression tests DIN EN 1052–1 [22] explicitly postulates the determination of the

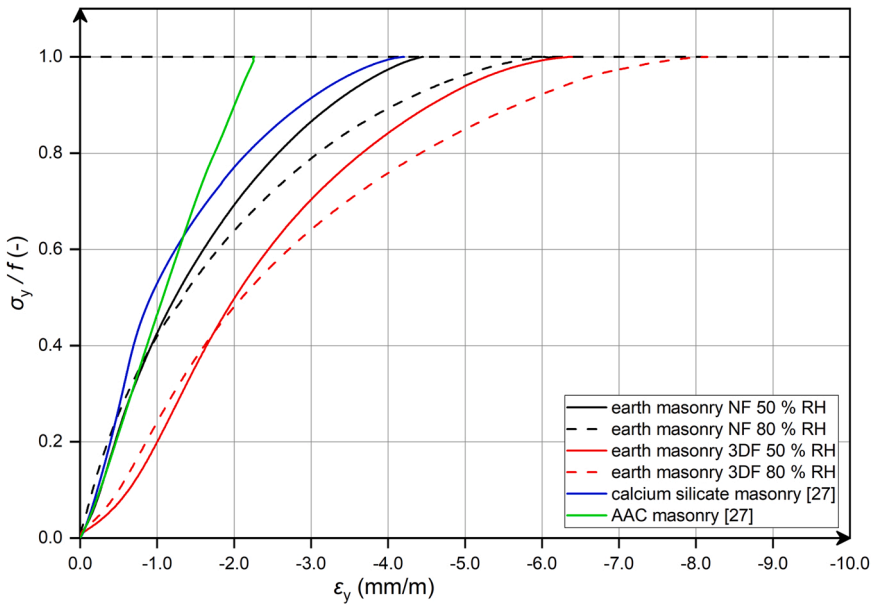

Fig. 13. Comparison of normalised stress-strain relations of earth block masonry, AAC masonry and calcium silicate masonry.

Table 5
Material parameters of earth blocks and mortars compared to calcium-silicate and AAC units and an M2.5 cement mortar (coefficient of variation in brackets).

block	RH (%)	compressive strength f_b (MPa)	Young's modulus E_{33} (MPa)	Poisson ratio ν_{33} (dimensionless)
NF	50	4.38 (6 %)	2735 (7 %)	0.17 (5 %)
	80	3.30 (3 %)	1629 (4 %)	0.10 (10 %)
3DF	50	5.38 (3 %)	3612 (15 %)	0.44 (2 %)
	80	3.55 (3 %)	1761 (1 %)	0.19 (51 %)
AAC*	–	4.90 (2 %)	2033 (4 %)	0.11 (13 %)
calcium silicate*	–	29.70 (7 %)	9310 (7 %)	0.12 (18 %)
earth mortar**	50	4.11 (2 %)	5559 (5 %)	0.12 (5 %)
	80	3.01 (1 %)	3570 (23 %)	0.12 (14 %)
M2.5*	–	2.60 (2 %)	4915 (2 %)	0.18 (11 %)

* results from [27].
** averaged values from M2 and M3.

Young's modulus as secant modulus. The distinctive non-linear stress-strain behaviour with post peak strain softening in general corresponds to the behaviour of masonry made of calcium silicate units [28] and is illustrated by means of the normalised stress-strain curves in Fig. 13. The stress-strain behaviour of the AAC masonry in contrary is almost linear until failure occurs and exhibits comparatively low strains at maximum stress. In Table 6 the characteristic values of earth block masonry obtained in this study and from literature as far as available are summarised and compared to values of conventional masonry. The characteristic masonry strength f_k of the earth block masonry specimens was determined according to DIN EN 1052–1 [22] by dividing the mean masonry strength f by 1.2. The coefficient α_0 describes the nonlinearity of the stress-strain curve until maximum stress and corresponding strain at maximum stress ε_f and is determined according to the following equation.

$$\alpha_0 = 1 \Big/ (\varepsilon_f * f) * \int_0^{ef} \sigma(\varepsilon) d\varepsilon$$

Apart from the general dependence on RH, the low ratio of E_{33}/f_k and the rather high strain at maximum stress constitute the main differences between earth and conventional masonry. In case of the 3DF masonry, the initial compaction phase leads to a high strain at maximum stress and causes the low E_{33}/f_k ratio as well as the low Poisson ratio. In accordance with the flattening of the curves and the increase of the strain at maximum stress at higher RH the α_0-values also increase slightly for earth block masonry. However, it stays within the same spectrum as masonry made of calcium silicate units. Furthermore, the E_{33}/f_k ratio is largely independent of RH, which simplifies the structural design significantly. Fig. 13 shows a comparison of the stress-strain relation of earth block masonry, AAC masonry and masonry made of calcium silicate units. The stress axis is normalised by the respective compressive strength of the different masonry types.

The masonry compressive strength according to DIN EN 1996–1–1 [15] is calculated by means of an exponential function in dependence of the block and mortar strength class. In Table 7 the masonry compressive strength calculated on this basis, using the parameters of solid blocks is compared with the characteristic earth block masonry strength determined from the test results assuming a coefficient of variation of 17 %, which is common for masonry made of fired bricks [30]. As a result, it can be seen, that the determination of earth block masonry's compressive strength yields consistent values at standard climate conditions (23 °C/50 % RH).

3. Conclusions

The dependence of the compressive strength and the Young's modulus of unstabilised earth block masonry and its components on

Table 6
Comparison of characteristic values of earth block masonry examined in this study and from literature with conventional masonry made from AAC and calcium silicate blocks.

Masonry	RH (%)	E_{33}/f_k (dimensionless)	ν_{33} (dimensionless)	ε_f (mm/m)	α_0 (dimensionless)
NF-masonry	50	497	0.13	4.4	0.65
(earth)	65	583	0.14	5.2	0.70
	80	563	0.10	6.4	0.71
3DF-masonry (earth)	50	283	0.07	6.3	0.64
	65	303	0.02	7.0	0.66
	80	308	0.10	8.1	0.68
Müller [14]	50	430–500	n.d.	3.2–7.1	n.d.
Miccoli [16,17]	50	245	0.37	2.1–6.3	n.d.
AAC*	–	500–650	0.17 – 0.32	1.4–3.7	0.53–0.60
calcium silicate*	–	800–1250	0.07 – 0.12	1.3–3.9	0.57–0.75
vertically perforated fired clay bricks *	–	950 – 1250	0.05 – 0.23	1.0–2.6	0.51–0.65

* results from [29].
n.d. = not determined

Table 7
Comparison of the calculated characteristic compressive strength acc. to DIN EN 1996–1–1 [15] with the experimental results assuming a CoV of 17 % combined per masonry type.

Masonry type	f_b block CS class 3 (MPa)	f_m mortar CS class 2.5 (MPa)	parameters of masonry compressive strength f_k for solid blocks acc. [15,23]			$f_{k,\ calculated}$ (MPa)	$f_{exp,\ CoV\ 0.17}$ (MPa)
			K (dimensionless)	α (dimensionless)	β (dimensionless)		
NF	3.8	2.5	0.95	0.585	0.162	2.41	2.58
3DF						2.41	2.50

the ambient relative humidity has to be considered during structural design. At a standard climate condition of 23 °C and 50 % RH, compressive strength and Young's modulus of unstabilised earth block masonry are comparable to the parameters of AAC masonry. The strain at maximum stress of earth block masonry especially at elevated levels of relative humidity is rather high in comparison to conventional masonry. The ratio between the Young's modulus and the compressive strength, however, is largely independent of relative humidity, which crucially simplifies the structural design. Furthermore, the production method and material composition influence the mechanical behaviour of unstabilised earth masonry. Microstructural texture effects caused by the extrusion lead to a pronounced compaction and elevated transversal strains under compression in case of the masonry made from extruded blocks. However, the strength and deformation characteristics of the unstabilised earth block masonry tested, even at a high level of 80 % ambient RH, are sufficient for masonry structures with a low number of storeys and the mechanical behaviour is in general comparable to conventional masonry. The structural design of earth block masonry can thus be made according to conventional masonry, if the influence of the relative humidity and the rather low Young's modulus are considered. Further research is needed to evaluate the influence of bending loads under eccentric compression as well as detailed investigations on the long-term material behaviour.

Declaration of Competing Interest

The authors declare that they have no known competing financial interests or personal relationships that could have appeared to influence the work reported in this paper.

Data Availability

Data will be made available on request.

Acknowledgement

This research was funded by Deutsche Bundesstiftung Umwelt (DBU) under reference number AZ 34599/01. The authors wish to acknowledge Mr. Markus Graubohm for providing data on masonry made of calcium-silicate and AAC units from his intense research in the field.

References

[1] E. Elhacham, L. Ben-Uri, J. Grozovski, Y.M. Bar-On, R. Milo, Global human-made mass exceeds all living biomass, Nature 588 (2020) 442–444, https://doi.org/10.1038/s41586-020-3010-5.
[2] R. Kajaste, M. Hurme, Cement industry greenhouse gas emissions–management options and abatement cost, J. Clean. Prod. 112 (2016) 4041–4052, https://doi.org/10.1016/j.jclepro.2015.07. 055.
[3] T. Held, M. Waltersbacher, Wohnungsmarktprognose 2030, BBSR-Anal. KOMPAKT 07 (2015).
[4] R. Braun, Wohnungsmarktprognose 2019–22: Regionalisierte Prognose in drei Varianten mit Ausblick bis 2030, Empirica-Paper 244, 2019.
[5] P. Deschermeier, R. Henger, B. Seipelt, M. Voigtländer, Wohnungsmarkt: politische Implikationen des zukünftigen Baubedarfs, IWPerspektive 2035 (2017) 197–206.
[6] T. Baldenius, S. Kohl, M. Schularick, Die Neue Wohnungsfrage: Gewinner und Verlierer des Deutschen Immobilienbooms, Leviathan 1 (2020).
[7] Statistisches Bundeasamt, Bautätigkeit und Wohnungen 2020 – Fachserie 5 Reihe 1 (2021).
[8] B.V.V. Reddy, et al., Codes and standards on earth construction, in: A. Fabbri, J.C. Morel, J.E. Aubert, Q.B. Bui, D. Gallipoli, B.V. Reddy (Eds.), Testing and Characterisation of Earth-based Building Materials and Elements. RILEM State-of-the-Art Reports, 35, Springer, Cham, 2022, https://doi.org/10.1007/978-3-030-83297-1_7.
[9] U. Röhlen, F. Volhardt, Lehmbau-Regeln: Begriffe – Baustoffe - Bauteile, third ed. Vieweg Teubner, Wiesb. (2009).
[10] P. Wiehle, S. Simon, J. Baier, L. Dennin, Influence of relative humidity on the strength and stiffness of unstabilised earth blocks and earth masonry mortar, Constr. Build. Mater. 342 (2022) 1–15, https://doi.org/10.1016/j.conbuildmat.2022.128026.
[11] A. Heath, P. Walker, C. Fourie, M. Lawrence, Compressive Strength of Extruded Unfired Clay Masonry Units, in: Proceedings of the Institution of Civil Engineers - Construction Materials Volume 162, Issue 3, 2009, pp. 105–112. https://doi.org/10.1680/coma.2009.162.3.105.
[12] DIN EN1995-1-1.:2010-12. Eurocode 5: Design of timber structures - Part 1–1: General - Common rules and rules for buildings; German version EN 1995–1-1: 2004 + AC:2006 + A1:2008.
[13] DIN 18945:2018-12. Earth blocks – Requirements, test and labelling.
[14] P. Müller, L. Miccoli, P. Fontana, C. Ziegert, Development of partial safety factors for earth block masonry, Mater. Struct. 50 (2017) 1–14, https://doi.org/10.1617/s11527-016-0902-9.
[15] DIN EN 1996-1-1:2013-02. Eurocode 6: Design of masonry structures – Part 1–1: General rules for reinforced and unreinforced masonry structures; German version EN 1996–1-1:2005 + A1: 2012.

[16] L. Miccoli, U. Müller, P. Fontana, Mechanical behaviour of earthen materials: A comparison between earth block masonry, rammed earth and cob, Constr. Build. Mater. 61 (2014) 327–339, https://doi.org/10.1016/j.conbuildmat.2014.03.009.
[17] L. Miccoli, A. Garofano, P. Fontana, U. Müller, Experimental testing and finite element modelling of earth block masonry, Eng. Struct. 104 (2015) 80–94, https://doi.org/10.1016/j.engstruct.2015.09.020.
[18] A. Heath, M. Lawrence, P. Walker, C. Fourie, The compressive strength of modern earth masonry, in: Bath, UK: 11thInternational Conference on Non-conventional Materials and Technologies, NOCMAT, 2009.
[19] DIN 18946: 2018–12. Earth masonry mortar – Requirements, test and labelling.
[20] P. Schubert, Prüfverfahren für Mauerwerk, Mauersteine und Mauermörtel, in: P. Funk (Ed.), Mauerwerk-Kalender 16, Verlag für Architektur und technische Wissenschaften, Berlin, 1991, pp. 685–697.
[21] DIN 18555–4: 2019–04. Testing of mortars containing mineral binders - Part 4: Determination of linear and transverse strain and of deformation characteristics of hardened masonry mortars by the static pressure test.
[22] DIN EN 1052-1:1998-12. Methods of test for masonry – Part 1: Determination of compressive strength, German version.
[23] DIN EN 1996-1-1/NA: 2019-12. National Annex – Nationally determined parameters – Eurocode 6: Design of masonry structures – Part 1–1: General rules for reinforced and unreinforced masonry structures, 2012.
[24] K.J. Krakowjak, P.B. Lourenco, F.J. Ulm, Multitechnique investigation of Extruded Clay Brick Microstructure, J. Am. Ceram. Soc. 94 (2011) 3012–3022, https://doi.org/10.1111/j.1551-2916.2011.04484.x.
[25] J. Bourret, N. Tessier-Doyen, R. Guinebretiere, E. Joussein, D.S. Smith, Anisotropy of thermal conductivity and elastic properties of extruded clay-based materials: evolution with thermal treatment, Appl. Clay Sci. 116 – 117 (2015) 150–157, https://doi.org/10.1016/j.clay.2015.08.006.
[26] A. Viani, R. Švečik, M.-S. Appavou, A. Radulescu, Evolution of fine microstructure during firing of extruded clays: a small angle neutron scattering study, Appl. Clay Sci. 166 (2018) 1–8, https://doi.org/10.1016/j.clay.2018.09.002.
[27] M. Graubohm, Einfluss des Kontakts zwischen Mauerstein und Mauermörtel auf das Drucktragverhalten von Mauerwerk, Dissertation, RWTH Aachen Univ. (2019), https://doi.org/10.18154/RWTH-2018-230286.
[28] W. Jäger, T. Vassilev, T. Pflücke, Ein neues Materialgesetz zur wirklichkeitsnahen Beschreibung des Baustoffverhaltens von Mauerwerk, Mauerwerk 8 Nr. 4 (S) (2004) 159–165, https://doi.org/10.1002/dama.200490058.
[29] W. Brameshuber, Eigenschaften von Mauersteinen, Mauermörtel, Mauerwerk und Putzen, in: W. Jäger (Ed.), Mauerwerk Kalender, Ernst und Sohn, Berlin, 2017, 2017, pp. 3–29, https://doi.org/10.1002/9783433607565.ch1.
[30] JCSS Probabilistic Model Code – Part 3: Material properties, Joint Committee on Structural Safety, 2001.